

# Ultralow thermal conductivity of a packed bed of crystalline nanoparticles: A theoretical study

Ravi Prasher\*

Intel Corporation, CH5-157, 5000 W. Chandler Blvd., Chandler, Arizona 85226-3699, USA

and Department of Mechanical &amp; Aerospace Engineering, Arizona State University, Tempe, Arizona 85287, USA

(Received 6 June 2006; revised manuscript received 24 August 2006; published 24 October 2006)

Theoretical thermal conductivity of a packed bed of crystalline spherical nanoparticles is reported. Thermal conductivity is dominated by surface and constriction thermal resistances and surface energy of the nanoparticles. Depending on the surface energy and size of the nanoparticles, thermal conductivity of the solid phase can be smaller than the minimum thermal conductivity given by the Einstein limit. It is also shown that depending on the surface energy and size of the nanoparticles, thermal conductivity of the nanoparticle bed can be smaller than the thermal conductivity of air. The range of surface energies under which these conditions are achievable for silicon-based nanoparticle beds is reported. Finally, it is shown that nanoconstrictions are more efficient in reducing thermal conductivity than superlattices and nanowires.

DOI: 10.1103/PhysRevB.74.165413

PACS number(s): 81.07.Wx, 82.60.Qr, 65.80.+n

## I. INTRODUCTION

The lowest possible thermal conductivity ( $k$ ) of solids is given by the Einstein limit ( $k_E$ ),<sup>1</sup> where the mean free path (mfp) is assumed to be the same as half the wavelength of the phonons. This model has been very successful in explaining thermal conductivity of amorphous solids.<sup>1</sup> For most solids at room temperature ( $T$ ) or higher the dominant phonon half wavelength is close to the lattice constant ( $b$ ). Therefore, at higher  $Tk_E=1/3b\sum_3\int c_\omega v_\omega d\omega$ , where  $c$  is the frequency-dependent heat capacity per unit volume,  $v$  the frequency-dependent group velocity, and  $\omega$  is the frequency of phonons. The last decade has seen enormous research in reducing the  $k$  of crystalline semiconductor solids using nanostructures for applications ranging from high-efficiency thermoelectric to microsensors.<sup>2</sup> Nanostructures investigated in the literature can be broadly categorized into thin films, superlattices, nanowires, and nanocomposites.<sup>2</sup> These nanostructures have very small  $k$  at room  $T$ ; however, it is much higher than  $k_E$ . To achieve  $k$  as small as  $k_E$  in crystalline nanostructures at room  $T$ , the size of the nanostructure has to be approximately as small as the lattice constant, which is not possible for the nanostructures mentioned above.

In this paper we theoretically calculate  $k$  of different nanoscale architecture: packed bed of spherical crystalline nanoparticles (NPs) in the presence of air (Fig. 1). We show that depending on the size and the surface energy of the NPs, it is possible to achieve  $k < k_E$  for the solid phase due to filtering of phonons at the interface of the two nanoparticles. We also show that depending on the size and the surface energy of the NPs, effective  $k$  of the solid phase and the gas phase (air) combination can be smaller than  $k$  of the gas. Technologies such as high-temperature energy storage tanks, gas turbine engines, and space applications require insulation with solidlike mechanical behavior<sup>3</sup> but  $k$  as small as possible. The packed bed of spheres is also important in technologies<sup>4</sup> such as packed bed catalytic reactors, automotive catalytic converters, and the thermal process of oil recovery. Knowledge of  $k$  is very important for these applications. Limited experimental work<sup>5</sup> already indicates that it is possible to make a packed bed of NPs.

## II. THEORETICAL FORMULATION

Figure 1 shows a spherical nanoparticle bed (NB) arranged in simple cubic pattern. The top and bottom substrates are not included in the thermal analysis. Due to the periodicity of the NB, the thermal problem reduces to finding the  $k$  of a unit cell. Figure 1(b) shows the top view of the unit cell which is composed of a cylindrical region. The side view shown in Fig. 1(c) shows that the cylindrical region.  $k$  of the NB is given by  $k_{NB}=\pi/4k_{cyl}+(1-\pi/4)k_{air}$ , where  $k_{cyl}$  is the

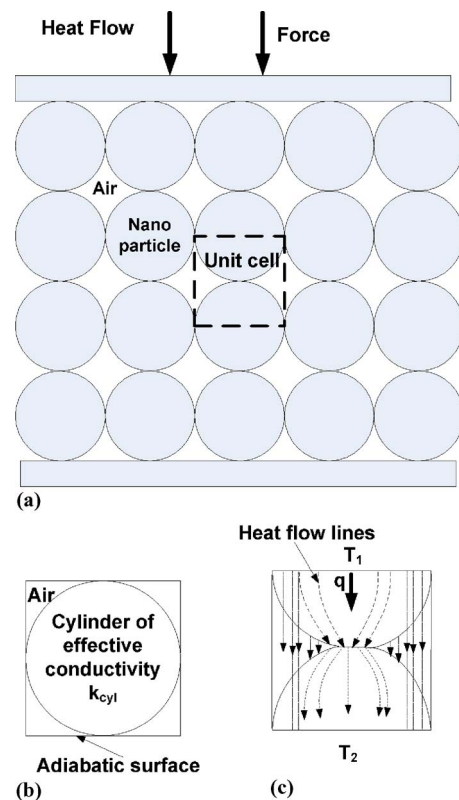


FIG. 1. (Color online) (a) Schematic of a packed bed of crystalline nanoparticles arranged in simple cubic pattern. (b) Top view of unit cell to compute  $k$ . (c) Cylindrical geometry to calculate  $k_{cyl}$  of the cylinder formed by air and the nanoparticle.

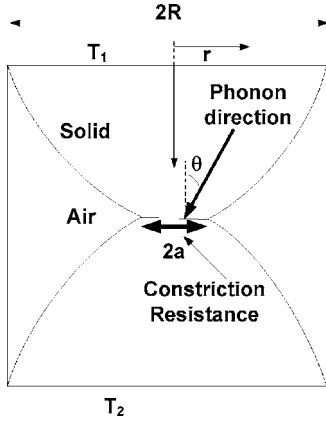


FIG. 2. Details of the geometry and the thermal problem to calculate  $k_{cyl}$  for the cylindrical geometry of Fig. 1(c) made of nanoparticle and air.

$k$  of the cylinder shown in Fig. 1(c). In writing this equation we have assumed no reduction in  $k$  of air surrounding the cylindrical region. This is possible if the boundary between air and the spheres is specular. For a diffuse interface  $k_{air}$  will decrease. Therefore  $k_{NB}$  in reality can be smaller. While calculating  $k_{cyl}$ , the size effects on  $k_{air}$  are included by including the thermal boundary resistance ( $R_b$ ) between air and the solid sphere. Figure 2 shows the cylindrical region in details. Due to application of external pressure ( $P$ ) and the presence of adhesion, a small circular constriction forms between two NPs.<sup>7</sup>  $R$  and  $a$  are the radius of the particle and the constriction, respectively.

For the size of the nanoparticles considered in the study we found that contribution of the thermal transport in the bulk of the solid and the gas is negligible compared to the interface thermal resistances, i.e., thermal transport is primarily ballistic in nature. Therefore, in this paper only the ballistic component is included in the analysis. As shown in Fig. 1(c), there are two parallel paths for heat transfer: (i) solid-to-solid through the air and (ii) solid-to-solid through the constriction formed by the two spheres. For  $a \gg l$ , where  $l$  is the mfp of phonons, the constriction resistance ( $\Lambda_c$ ) is modeled using Maxwell's formula,<sup>4,6</sup>  $\Lambda_{Maxwell} = 1/2ka$ . For NB,  $a$  will be very small. In the other limit of  $a \ll l$ , phonon transport through the constriction will be ballistic. The heat transfer rate,  $Q$ , in the ballistic limit can be written as

$$Q = \frac{1}{2} \left[ \sum_3 \int_{\omega=0}^{\omega=\omega_m} \int_{\theta=0}^{\theta=\pi/2} \frac{\hbar \omega}{\exp(\hbar \omega / k_b T) - 1} \times D_\omega \nu_\omega \tau(\omega, \theta) \sin \theta d\theta d\omega \right] A, \quad (1)$$

where  $A$  is the area of the constriction,  $\omega_m$  the maximum frequency,  $\nu$  the phonon group velocity,  $D$  the density of states/volume, and  $\tau$  is the transmissivity of phonons. The summation indicates three polarizations of phonons. For small differences in  $T$  on two sides, the ballistic constriction resistance,  $\Lambda_b$ , is given by

$$\frac{1}{\Lambda_b} = \frac{\partial Q}{\partial T} = \frac{1}{2} \left[ \sum_3 \int_{\omega=0}^{\omega=\omega_m} \int_{\theta=\pi/2}^{\theta=\pi/2} c_\omega \nu_\omega \tau(\omega, \theta) \sin \theta d\theta d\omega \right] A. \quad (2)$$

Equation (2) assumes bulk phonon dispersion of three-dimensional solid. Due to the small size of the NPs the dispersion relation can deviate from bulk phonon dispersion.<sup>2</sup> The dispersion relation will deviate from bulk dispersion if the NP size is comparable to the dominant wavelength ( $\lambda_D$ ) of the thermally excited phonons.  $\lambda_D$  can be written as<sup>2</sup>  $\hbar \omega_D = 2\pi \hbar v / \lambda_D = k_b T$ . Change in the phonon dispersion from the bulk can be estimated based on solving the wave equation in a freestanding NP in air. Calculations have been performed for silicon (Si) based NB. Since the mass density of air  $\ll$  mass density of Si, the appropriate boundary condition is a stress-free surface. Nakayama *et al.*<sup>8</sup> considered this case to calculate  $R_b$  between NP and liquid helium at  $T < 1$  K. They showed that for  $R/\lambda_D > 0.5$ ,  $R_b$  obtained from the solution of the wave equation with stress-free boundary condition reduced to  $R_b$  given by assuming bulk dispersion. Similarly Nakamura *et al.*<sup>8</sup> showed that  $R_b$  between NPs (diameter: 7 nm–40 nm, T: 5 K–200 K) and polyethylene could be well described by assuming bulk phonon dispersion. At room  $T$ ,  $\lambda_D$  of Si is  $\sim 1$  nm.<sup>2</sup> Considering this bulk phonon dispersion has been assumed as calculations have been performed for NP diameter  $> 5$  nm.

Although  $R \gg \lambda_D$ ,  $a$  can be comparable to  $\lambda_D$  ( $a \ll R$ ), leading to diffraction effects.  $\tau$  can be obtained by solving the wave equation through the circular aperture formed by the constriction assuming stress-free boundary conditions at the NP/air interface. For  $a \ll R$ ,  $\tau$  can be obtained by considering a plane screen (with stress-free boundary) separating the two half spaces and using spheroidal wave functions.<sup>9</sup> In the geometrical scattering, i.e., for  $a \gg \lambda_D$ ,  $\tau =$  the ratio of the projected area of the constriction in the direction of the incident wave and the real area of the constriction, i.e.,  $\tau = \cos \theta$ . For this case Eq. (2) gives

$$1/\Lambda_b = 1/4 \left[ \sum_3 \int_{\omega=0}^{\omega=\omega_m} c_\omega \nu_\omega d\omega \right] A. \quad (3)$$

For  $T \ll$  Debye  $T$ , Eq. (3) reduces

$$1/\Lambda_b = A \times \pi^2/30 \times (k_b^4/\hbar^3) (\nu_L^{-2} + 2\nu_T^{-2}) T^3, \quad (4)$$

where  $\nu_L$  and  $\nu_T$  are the longitudinal and transverse phonon velocity. Schwab *et al.*<sup>2</sup> measured the conductance of silicon nitride catenoidal nanowire at very low  $T$ . The minimum cross-sectional area of their catenoidal nanowire was 60 nm  $\times$  200 nm. Minimum area in the catenoidal wire acts like a constriction to heat flow. Figure 3 shows the comparison<sup>10</sup> between Eq. (4) and their data using  $A = 60$  nm  $\times$  200 nm. Equation (4) matches very well with data for  $T \geq 0.8$  K. For  $T < 0.8$  K the conductance reduces to the universal quantized conductance ( $g_0 = \pi^2 k_b^2 T / 3h$ ) of a one-dimensional mesoscopic conductor due to severe deviation in phonon dispersion from the bulk dispersion.  $\lambda_D$  for silicon nitride at  $T = 0.8$  K is 432 nm, which is much larger than the size of the minimum cross section. This shows that assuming

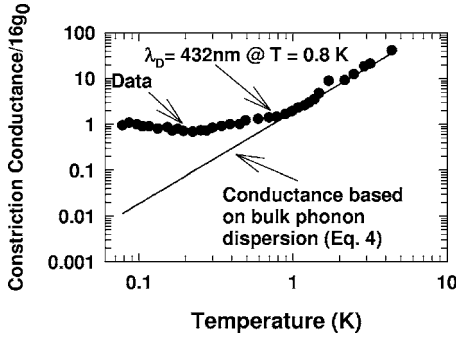


FIG. 3. Comparison between experimental data by Schwab *et al.*<sup>2</sup> on the conductance of a catenoidal wire and a three-dimensional constriction conductance given by Eq. (6). Minimum cross-sectional area of the wire behaves like a constriction. Phonon dispersion changes from bulk only for wire dimension  $< \lambda_D$ .  $\lambda_D$  at  $T=0.8$  K is 432 nm.

bulk dispersion is a good assumption for most of the temperature range and particularly for room  $T$ . In the limit of  $a \ll \lambda_D$ ,  $\tau$  can be calculated from the Rayleigh formula.<sup>9</sup> In the Rayleigh limit,  $\tau_{Ray} = 8/(27\pi^2)(\omega a/v)^4(\cos \theta)^2$  for a circular constriction, which leads to

$$1/\Lambda_b = 128/1215 \times \pi^3 a^6 (k_b^8/\hbar^7)(v_L^{-6} + 2v_T^{-6})T^7 \quad (5)$$

for  $T \ll$  Debye  $T$ . Equation (5) is the conductance of a very small abrupt constriction formed between two three-dimensional bodies assuming bulk phonon dispersion. Equation (5) shows that at very low  $T$ ,  $\Lambda_b$  is proportional to  $a^{-6}$ , which makes  $\Lambda_b$  very large compared to that given by Eq. (4) or the Maxwell formula. We found that room  $T$ ,  $\Lambda_b$  is very well described by Eq. (3).

$R_b$  at the air-solid interface is important for the NPs.  $R_b$ , expressed in the units of impedance for the air-solid interface, can be written as<sup>4</sup>

$$R_{b,air} = 2[(2 - \beta)/\beta][2/(\psi + 1)][(1/(\mu C_v))]l_{air}, \quad (6)$$

where  $\beta$  is the accommodation coefficient,  $l_{air}$  the mfp of air molecules,  $\psi$  the ratio of specific heats,  $\mu$  the viscosity of the gas, and  $C_v$  is the specific heat of air at constant volume.  $\beta$  depends on the acoustic properties of the solid and the gas.<sup>11</sup>  $\beta$  for air<sup>4</sup> is typically 0.9. In engineering literature<sup>4</sup> the same phenomenon at the gas-solid interface is referred to as temperature-jump-distance (TJD) or temperature slip length due to ballistic transport of air molecules in small geometries. Dharmadurai<sup>11</sup> showed that treating the problem from the point of view of  $R_b$  based on an acoustic mismatch model or TJD are equivalent. At ambient conditions,  $R_{b,air} = 4.9 \times 10^{-6} \text{ K m}^2 \text{ W}^{-1}$ . It can be shown that  $TJD = R_{b,air} \times k_{air} = 128 \text{ nm}$  (Kapitza length) at ambient conditions. Expressed in terms of conductance,  $G_{b,air} \approx 0.25 \text{ MW m}^{-2} \text{ K}^{-1}$ . At room  $T$ ,  $G$  of the solid-solid<sup>11</sup> interface is  $\sim 100 \text{ MW m}^{-2} \text{ K}^{-1}$  and liquid-solid interface is  $\sim 10 \text{ MW m}^{-2} \text{ K}^{-1}$ .  $G$  for the liquid-solid interface is one order of magnitude smaller than the solid-solid interface due to larger mismatch in acoustic properties. Similarly,  $G$  of the solid-air interface is one order of magnitude smaller than the solid-liquid interface due to larger mismatch in acoustic properties as compared to the

solid-liquid interface. The contribution of radiation heat transfer between the two spheres is also assessed. Due to the closeness of the NPs, the wavelength of the photons can be comparable to the air-gap thickness, making the near-field effects important.<sup>12</sup> An upper-bound estimate<sup>12</sup> for the near field can be made for dielectrics such as intrinsic Si by using  $G_{rad} = 4n^2\sigma T^3 \times 2\pi R^2$ , where  $n$  is the refractive index of Si and  $\sigma$  is the Stefan-Boltzmann constant. The effect of radiation was found to be negligible.

The effective thermal resistance of the solid-air combination is given by

$$1/\Lambda_{cyl} = \pi R^2/(2R_{b,air}) + 1/\Lambda_b = \pi R^2 k_{cyl}/(2R), \quad (7)$$

which using Eq. (3) leads to

$$k_{cyl} = R/R_{b,air} + 0.5a^2/R \sum_3 \int c_\omega v_\omega d\omega. \quad (8)$$

In Eq. (8) the first term is the contribution of air and second term is the contribution of solid.

In the macroscopic treatment of packed beds,  $a$  is given by Hertzian contact analysis,<sup>4</sup> which leads to  $a = (0.75FR^*/E^*)^{1/3}$ , where  $F$  is the force,  $R^* = R_1R_2/(R_1+R_2)$ , where  $R_1$  and  $R_2$  are the radius of the two spheres and  $E^{*-1} = (1-\nu_1^2)/E_1 + (1-\nu_2^2)/E_2$ , where  $E$  is the Young's modulus and  $\nu$  is the Poisson's ratio. If the pressure applied at the top substrate is  $P$ , then the force on each sphere is  $F = \pi R^2 P$ , leading to  $a = (0.375\pi P/E^*)^{1/3}R$ . For small particles, microscopic adhesive surface forces play a very dominant role.  $a$ , including the surface force, is modeled using the well-known JKR theory.<sup>7</sup> The effective force is given by  $F_{eff} = F + 3\gamma\pi R^* + \sqrt{6\gamma\pi R^*F + (3\gamma\pi R^*)^2}$ , where  $\gamma$  is the work of adhesion per unit area.  $\gamma$  is given by<sup>13</sup>  $\gamma = \gamma_1 + \gamma_2 - \gamma_{12}$ , where  $\gamma_1$  and  $\gamma_2$  are the surface energy per unit area of materials 1 and 2, and  $\gamma_{12}$  is the interface energy per unit area. If two materials are the same then  $\gamma = 2\gamma_1$ . In the absence of external force,  $a$  solely due to adhesion is given by  $a_0 = (1.125\pi\gamma/E^*)^{1/3}R^{2/3}$ .

### III. RESULTS AND DISCUSSION

The calculations have been performed for Si-based NB. Before discussing the results, the range of  $\gamma_1$  of Si is briefly discussed. For a detailed discussion readers are referred to the book by Q.-Y. Tong and U. Gösele.<sup>13</sup>  $\gamma_1$  is a strong function of surface treatment, surface contaminant, absorbed layers of other molecules such as water, and the annealing (bonding) temperature.  $\gamma = 2\gamma_1$  is the same as the fracture energy for monolithic material such as single-crystal Si.  $\gamma_1$  for clean Si is of the order of  $1000 \text{ mJ m}^{-2}$ .<sup>13</sup> For a surface exposed to the ambient,  $\gamma_1$  can drop significantly because the surface may absorb species from the ambient.  $\gamma_1$  for an exposed surface is also a strong function of the bonding (annealing) temperature. Depending on the surface treatment and annealing temperature, the range of  $\gamma_1$  of Si observed in the literature is  $1 \text{ mJ m}^{-2} - 1000 \text{ mJ m}^{-2}$ .<sup>13</sup> The upper limit corresponds to clean Si or contaminated-chemically treated Si at very high annealing temperatures, and the lower limit corresponds to hydrophobic Si at low temperatures. There-

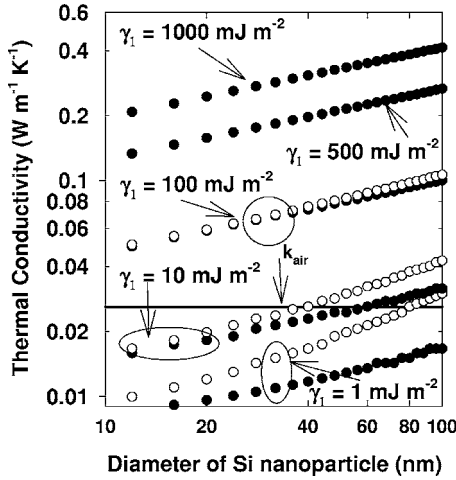


FIG. 4. Thermal conductivity of NB as a function of nanoparticle size, surface energy, and external pressure.  $k$  is a strong function of nanoparticle size and surface energy. Effect of pressure depends on the surface energy (filled circles:  $P=0$ ; unfilled circles:  $P=6.9 \times 10^9$  Pa). At high surface energy the constriction size is dominated by the adhesion forces for smaller particles. Therefore pressure does not impact  $k$  much for large surface energy, whereas for small surface energy external pressure has large impact. (See text for details.)

fore calculations have been performed for  $\gamma_1$  ranging from  $1 \text{ mJ m}^{-2}$ – $1000 \text{ mJ m}^{-2}$  in the paper to clearly identify the regime where  $k$  of the NB can be smaller than  $k$  of air.

Figure 4 shows  $k$  of Si-based NB at room  $T$ .  $\Lambda_b$  from Eq. (3) is calculated using experimental phonon dispersion.<sup>14</sup> Data<sup>15</sup> indicates that  $E$  of nanostructured Si is the same as bulk  $E$ . Therefore  $E$  is assumed to be the same as  $E$  of bulk Si.<sup>16</sup>  $k$  is calculated for  $P=0$  and  $6.9 \times 10^5$  Pa (100 PSI). Note that if adhesion force is neglected, then for  $P=0$ ,  $a=0$ . Figure 4 shows that effective thermal conductivity of the nanoparticle bed ( $k_{NB}$ ) is very low for both very low and very high surface energy. The main reason that  $k_{NB}$  is very small is that for NPs,  $\Lambda_b$  is very large. The impact of  $R_b$  between air and the NP is also very large. With increasing NP size, the impact of  $\Lambda_b$  and  $R_{b,air}$  decreases, leading to an increase in  $k_{NB}$ . Figure 4 also shows that depending on the surface energy,  $k_{NB}$  can be lower than  $k$  of air. To achieve  $k$  smaller than  $k$  of air, the surface energy of NPs has to be relatively small ( $\gamma_1 \approx 10 \text{ mJ m}^{-2}$  or lower). For Si, this is possible only with surface treatment and low-temperature bonding.<sup>13</sup> However, even for surface energy as high as  $500 \text{ mJ m}^{-2}$ ,  $k_{NB}$  is comparable to  $k$  of typical polymers ( $\sim 0.2\text{--}0.3 \text{ W m}^{-1} \text{ K}^{-1}$ , Ref. 17), i.e., a packed bed of crystalline nanoparticles has  $k$  the same as  $k$  of polymers. Figure 4 also shows that for  $\gamma_1$  as high as  $1000 \text{ mJ m}^{-2}$  (corresponding to  $\gamma$ =fracture energy)  $k$  is still very small.

From Eq. (8), the contribution of solid phase is given by

$$k_{solid} = 1/2 \left( \sum_3 \int c_\omega v_\omega d\omega \right) a \times a/R. \quad (9)$$

Physical interpretation of Eq. (9) is that for an abrupt nanoconstriction,  $mfp \approx a$ ; however number of phonons crossing

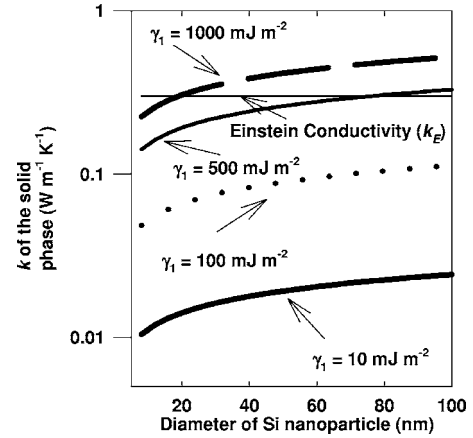


FIG. 5. Thermal conductivity of the solid phase as a function of nanoparticle size and surface energy for  $P=0$ .  $k_{solid}$  is a strong function of nanoparticle size and surface energy. For  $\gamma_1$  as high as  $1000 \text{ mJ m}^{-2}$ , which corresponds to  $\gamma$ =fracture energy of Si (possible for very clean Si), it is possible to achieve  $k_{solid} < k_E$ , however, only for very small NP. For  $\gamma_1$  as high as  $500 \text{ mJ m}^{-2}$ ,  $k_{solid} < k_E$  can be achieved for relatively larger NPs. (See text for details.)

the interface is reduced by  $a/R$ , i.e., filtering of phonons takes place. For geometries such as nanowires, thin films, and superlattices,  $a=R$ , i.e.,  $a/R=1$ . Therefore a nanoconstriction is more efficient in reducing  $k$  than nanowires, thin films, and superlattices. Equation (9) shows that the effective mfp of nanoconstriction is  $\sim a^2/R$ , which for pure Hertzian contact leads to  $l \propto (P/E^*)^{2/3} R$ , and for pure adhesive contact,  $l \propto (\gamma/E^*)^{2/3} R^{1/3}$ . Figure 5 shows  $k_{solid}$  for various values of  $\gamma_1$ . Using experimental phonon dispersion,<sup>14</sup> the Einstein conductivity ( $k_E$ )  $0.3 \text{ W m}^{-1} \text{ K}^{-1}$ . It is to be noted that this value is lower than that predicted by using the Debye model<sup>1</sup> because we have used the experimentally measured phonon dispersion, which leads to smaller group velocity and heat capacity of acoustic phonons at room  $T$  as compared to the Debye model.<sup>2</sup> Using the Debye model,  $k_E \sim 1 \text{ W m}^{-1} \text{ K}^{-1}$ , which is much closer to the experimental data on amorphous Si.<sup>1</sup> Figure 5 shows that depending on the surface energy and size of the NP,  $k_{solid}$  is smaller than  $k_E$ . Even for  $\gamma_1$  as high as  $1000 \text{ mJ m}^{-2}$  (corresponding to  $\gamma$ =fracture energy),  $k_{solid}$  can be smaller than  $k_E$ , however, only for very small NPs ( $< 20 \text{ nm}$ ). Although  $k_{solid}$  is higher than  $k_E$  for most of the range of NP sizes considered for larger values of  $\gamma_1$ , it is still smaller than  $k$  of amorphous Si ( $\sim 1 \text{ W m}^{-1} \text{ K}^{-1}$ ),<sup>1</sup> which means that by using crystalline NPs it is possible to achieve  $k$  smaller than the  $k$  of amorphous phase.

From Eq. (9),  $k_{solid}/k_E = 1.5(a/b)(a/R)$ . As long as  $a^2/R < b/1.5$ ,  $k_{solid} < k_E$ .  $a^2/R$  for purely adhesive contact is given by

$$a^2/R = (1.125\pi\gamma/E^*)^{2/3} R^{1/3} \quad (10)$$

Equation (10) shows that  $a^2/R$  is a stronger function of the surface energy than the size of the NP. Therefore reduction in the surface energy leads to larger reduction in  $k_{solid}$  as compared to the reduction in the size of the NPs. The key to reduce  $a^2/R$  is to significantly reduce the surface energy and

the size of the NPs. Reduction in surface energy can be achieved via surface treatment and using low-temperature bonding.<sup>13</sup>

#### IV. CONCLUSION

We have shown that with proper combination of NP size and surface energy, it is possible to achieve  $k$  in crystalline solids below the Einstein limit and lower than the  $k$  of the amorphous phase due to phonon filtering at the interface. Depending on the surface energy and size of the NPs, the effective  $k$  of a packed bed of NPs and gas can be smaller than  $k$  of the gas. To achieve this, low surface energy is required which can be achieved by chemically treating the surface and employing low-temperature bonding. This offers a great flexibility in designing materials. A packed bed of

NPs will behave like a solid from a mechanical point of view; however, effective  $k$  can be smaller than  $k$  of the gas, making NB an excellent candidate for highly effective insulators. NB can also be potentially used as high-performance thermoelectric due to enormous decrease in  $k$ . In this study we have considered the same nanoparticles; however, dissimilar nanoparticles can decrease  $k$  further due to reflection of the phonons because of mismatch in the acoustic properties, which will be explored later.

#### ACKNOWLEDGMENTS

We thank Tao Tong and Arun Majumdar of UC Berkeley for helpful discussions.

\*Electronic address: ravi.s.prasher@intel.com

<sup>1</sup>D. G. Cahill and R. O. Pohl, Phys. Rev. B **35**, 4067 (1987); Solid State Commun. **70**, 927 (1989).

<sup>2</sup>K. Schwab, E. A. Henriksen, J. M. Worlock, and M. L. Roukes, Nature (London) **404**, 974 (2000); Y. S. Ju and K. E. Goodson, Appl. Phys. Lett. **74**, 3005 (1999); P. K. Schelling and S. R. Phillpot, J. Appl. Phys. **93**, 5377 (2003); N. Mingo and D. A. Broido, Phys. Rev. Lett. **93**, 246106 (2004); D. Li, Y. Wu, P. Kim, L. Shi, P. Yang, and A. Majumdar, Appl. Phys. Lett. **83**, 2934 (2003); E. P. Pokatilov, D. L. Nika, and A. a. Balandin, Phys. Rev. B **72**, 113311 (2005); J. D. Chung and M. Kaviani, Int. J. Heat Mass Transfer **43**, 521 (2000); R. Yang and G. Chen, Phys. Rev. B **69**, 195316 (2004); R. S. Prasher, J. Appl. Phys. **100**, 034307 (2006).

<sup>3</sup>G. Soyez, J. A. Eastman, L. J. Thompson, G.-R. Bai, P. M. Baldo, A. W. McCormick, R. J. DiMelfi, A. A. Elmustafa, M. F. Tambwe, and D. S. Stone, Appl. Phys. Lett. **77**, 1155 (2000); H. L. Paul and K. R. Diller, J. Biomed. Eng. **125**, 639 (2003).

<sup>4</sup>C. V. Madhusudana, *Thermal Contact Conductance* (Springer, New York, 1995); G. Buonanno, A. Carotenuto, G. Giovinco, and N. Massarotti, J. Heat Transfer **125**, 693 (2003).

<sup>5</sup>D. Xia and S. R. J. Brueck, J. Vac. Sci. Technol. B **23**, 2694 (2005); P. Scheier, B. Marsen, and K. Sattler, J. Appl. Phys. **94**, 6069 (2003).

<sup>6</sup>G. Wexler, Proc. Phys. Soc. London **89**, 927 (1966); B. Nikolic and P. B. Allen, Phys. Rev. B **60**, 3963 (1999).

<sup>7</sup>K. L. Johnson, K. Kendall, and A. D. Roberts, Proc. R. Soc. London **324**, 301 (1971).

<sup>8</sup>T. Nakayama and N. Nishiguchi, Phys. Rev. B **24**, 6421 (1981); H. Nakamura, M. Matsuura, K. Kawasaki, Y. Hiki, and Y. Kogure, J. Appl. Phys. **79**, 3994 (1996).

<sup>9</sup>C. J. Boukamp, Rep. Prog. Phys. **17**, 35 (1954).

<sup>10</sup> $v_L=10070 \text{ m s}^{-1}$  and  $v_T=6450 \text{ m s}^{-1}$  assumed; See Y. Tanaka, F. Yoshida, and S. Tamura, Phys. Rev. B **71**, 205308 (2005).

<sup>11</sup>G. Dharmadurai, J. Appl. Phys. **54**, 5990 (1983); Phys. Status Solidi B **116**, 307 (1983); D. G. Cahill, W. K. Ford, K. E. Goodson, G. D. Mahan, A. Majumdar, H. J. Maris, R. Merlin, and S. R. Phillpot, J. Appl. Phys. **93**, 793 (2003); H. A. Patel *et al.*, Nano Lett. **5**, 2225 (2005).

<sup>12</sup>C. J. Fu and Z. M. Zhang, Int. J. Heat Mass Transfer **49**, 1703 (2006); J. L. Pan, K. H. Choy, and C. G. Fonstad, IEEE Trans. Electron Devices **47**, 241 (2000).

<sup>13</sup>Q.-Y. Tong and U. Gösele, *Semiconductor Wafer Bonding: Science and Technology* (John Wiley & Sons, New York, 1999); K. T. Turner, S. M. Spearing, W. A. Baylies, M. Robinson, and R. Smythe, IEEE Trans. Semicond. Manuf. **18**, 289 (2005); T. Martini, J. Steinkirchner, and U. Gösele, J. Electrochem. Soc. **144**, 354 (1997); Q.-Y. Tong, Q. Gan, G. Hudson, G. Fountain, P. Enquist, R. Scholz, and U. Gösele, Appl. Phys. Lett. **83**, 4767 (2003); R. Perez and P. Gumbsch, Phys. Rev. Lett. **84**, 5347 (2000).

<sup>14</sup>B. N. Brockhouse, Phys. Rev. Lett. **2**, 256 (1959).

<sup>15</sup>K. R. Virwani, A. P. Malshe, W. F. Schmidt, and D. K. Sood, Smart Mater. Struct. **12**, 1028 (2003); A. Heidelberg, L. T. Ngo, B. Wu, M. A. Phillips, S. Sharma, T. I. Kamins, J. E. Sader, and J. J. Boland, Nano Lett. **6**, 1101 (2006).

<sup>16</sup> $E$  of Si is crystal orientation dependent. For the calculations,  $E$  for [111] direction has been chosen in the paper.  $E=187 \text{ GPa}$ ,  $\nu=0.29$ . W. C. O'Mara, R. B. Herring, and L. P. Hunt, *Handbook of Semiconductor Silicon Technology* (William Andrew Publishing, Norwich, NY, 1990).

<sup>17</sup>J. Brandrup and E. H. Immergut, *Polymer Handbook* (John Wiley & Sons, New York, 1989).